American Journal of Computer Science and Information Engineering
2019; 6(1): 13-22
http://www.aascit.org/journal/ajcsie
ISSN: 2381-1110 (Print); ISSN: 2381-1129 (Online)

American Association for Science and Technology

Optimization of Liner Shipping Routes Considering Emission Control Area Based on Space-Time Network

Feng Pengjun

College of Transport & Communications, Shanghai Maritime University, Shanghai, China

Email address

fpjascend@163.com

Citation

Feng Pengjun. Optimization of Liner Shipping Routes Considering Emission Control Area Based on Space-Time Network. *American Journal of Computer Science and Information Engineering*. Vol. 6, No. 1, 2019, pp. 13-22.

Received: May 5, 2019; **Accepted**: June 16, 2019; **Published**: June 25, 2019

Abstract: In container liner shipping, fuel consumption directly related to speed brings huge operating costs to shipping companies. At the same time, due to the increasing awareness of environmental protection, ports in various countries have proposed port emission control areas (ECA), which also increased the operating costs of shipping companies. This paper comprehensively considers the factors of liner fuel consumption and emission control area, and optimizes the liner route. By using the space-time network framework, a three-dimensional network model of "space-time-speed" (STS) is constructed by introducing the velocity dimension. The speed is discretized with a reasonable step size, and a 0-1 integer programming model that minimizes operating costs is established. In addition, in the context of the emission control area, it is assumed that there are three alternative navigation options between any two ports in a route. Based on the space-time network model framework, the liner route selection and sailing speed are jointly optimized. In the empirical part, four routes provided by COSCO was selected to construct different ECA scenario cases for comparative analysis. The results show that the STS three-dimensional spatio-temporal network model framework constructed in this paper can effectively solve the liner route optimization problem and describe the liner transportation schedule in more detail.

Keywords: Waterway Transportation, Liner Route Optimization, Space-Time-Speed Network Model, Emission Control Area

1. Introduction

Container liner shipping plays a very important role in shipping and global logistics systems. UNCTAD assessed that the volume of global container ports increased by 42.3 million TEUs in 2017, reaching a total of 752.2 million TEUs [1]. In order to complete the transportation service, the consumption of marine fuel is indispensable, and the cost of purchasing fuel by the shipping company is the most important component of the company's operating costs. Moreover, With the introduction of the Emission Control Area (ECA) policy in various countries and regions, it is necessary to meet lower emission requirements within the ECA, the shipping company has to use lower-emission fuels during operations, further increasing the shipping company's operating costs [2-4]. Therefore, in considering the emission control area conditions and meeting the navigation time constraints, it is very necessary for the shipping company to choose the appropriate route and speed optimization.

There have been many research results on the route and speed optimization of liner shipping. As we all know, the fuel consumption in liner sailing is not only related to the design and structure of the ship, but also directly related to its sailing speed. Ronen (1982) believes that the daily fuel consumption of the liner is proportional to the cubic of the sailing speed [5]. Through the analysis of historical operational data of container liners, Wang and Meng (2012) further corrected the relationship between sailing speed and fuel consumption and found that the exponent was between 2.7 and 3.3 [6]. In terms of ship engine manufacturing, for feeder container ships, medium-sized container ships and giant container ships, Du et al. (2011) gave recommendations of 3.5, 4 and 4.5 respectively. In a sailing service, if the speed of navigation exceeds 20 knots, the index should be set to 4 [7].

In general, high sailing speeds result in higher annual cargo turnover and lower transportation inventory costs, while also consuming more fuel, which in turn leads to more transportation costs and gas emissions, such as greenhouse gases (carbon dioxide and nitrogen dioxide) and non-greenhouse gases (sulfur oxides and nitrogen oxides). These gases also have a huge negative impact on the global climate, such as greenhouse gases making global warming, acid rain from sulfur oxides corroding the earth's vegetation, etc., which is contrary to environmentally friendly development strategies [8-12]. Therefore, the International Maritime Organization (IMO) has proposed emission control areas to minimize emissions during transportation, such as the Baltic Sea, the North Sea-English Channel, North America and the US Caribbean Coast Emission Control Area [13]. China has also implemented the port emission control area policy since 2016, and specifically set up three pollutant emission control areas in the Yangtze River Delta, the Pearl River Delta and the Bohai Sea waters [14-15].

With the increasing awareness of environmental protection, both the shipping company and the research community have paid great attention to the compliance with ECA regulations. Schinas and Stefanakos (2012) proposed a stochastic programming model to determine the combination of fleets operating in the context of ECA [16]. Cullinane and Bergqvist (2014) pay more attention to the technical options that follow the ECA rules [17]. Jiang et al. (2014) through the economic analysis of the two methods of installing scrubbers and fuel replacement. According to the results of this study, mainly depends on the difference between Marine Gas Oil (MGO) and Heavy Fuel Oil (HFO) when choosing different methods [18]. Yang et al. (2012) conducted a detailed analysis and comparison of the three methods by considering a series of standards such as capital and operating costs, operational difficulty and maintenance requirements, and found that the fuel replacement method in the control of sulfur oxides has a big advantage, but in the face of externally more stringent emission limits, the installation of an exhaust gas scrubber is the best choice [19]. Brynolf et al. (2014) and Balland et al. (2012, 2013) comprehensively analyzed sulfur oxide compliance and NOx reduction [20-22].

In the context of ECA, how liners choose the best route to minimize their transportation costs is also one of the issues that ship companies need to consider. Cheng et al. (2017) comprehensively considered the ship type, the number of ships, the ship speed, the carbon tax and other factors, and established a sulfur emission control area and a carbon emission reduction liner route cost model. The results show that in the ECA context, in order to minimize costs, the liner will choose a lower speed to sail [14]. However, this study did not consider the existence of multiple route options between ports. Therefore, Fagerholt et al. (2015) constructed a liner route and speed optimization model by considering the sulfur emission control area to minimize operating costs, and analyzed the changes in operating costs when there were multiple route schemes between ports [23], but did not apply on the entire route.

Considering comprehension of the above literature, the main work of this paper is as follows. Firstly, in the context of ECA, the situation of multiple route options between any two ports is considered, and various options are jointly optimized to provide shipping companies with more detailed route options. Secondly, using the Space-Time-Speed (STS) network model framework, the complex nonlinear speed optimization problem is transformed into a simple 0-1 integer programming problem by discretizing the speed with reasonable step size to improve the efficiency of the model. Thirdly, combined with the time-sensitive of space-time network framework, these characteristics can obtain detailed timetables for liner transportation and improve the transportation efficiency of shipping companies.

2. Problem Description

Under the space-time network model, in order to facilitate the construction of the later optimization model, Figure 1 shows the schematic diagram of the "space-time-speed" (STS) three-dimensional network model for the liner service route, and illustrates the relevant definition of the model construction.

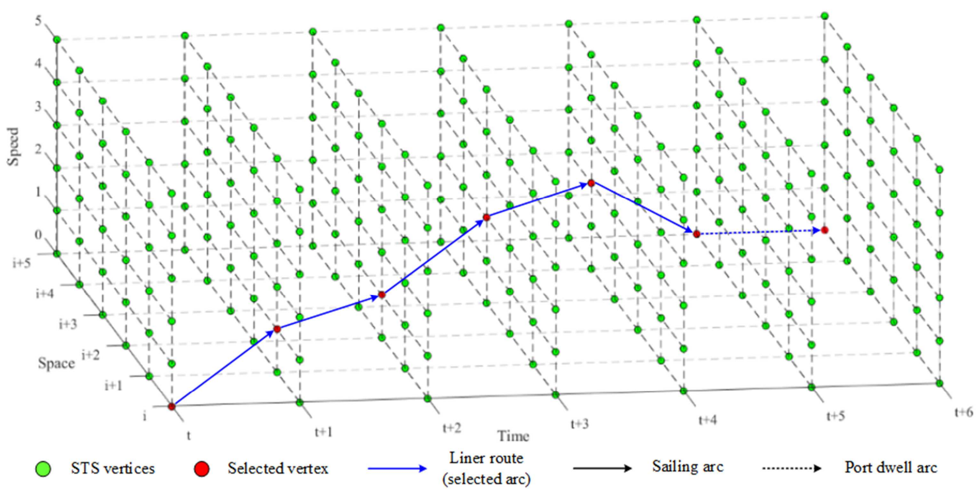

Figure 1. *Schematic diagram of the liner route under the space-time network.*

Figure 1 illustrates a feasible space-time network route between the port of i and the port of $i+5$, that is, the liner departs from port i at time t (the speed is 0 at the time of departure), and the speed at the time of arrival at $i+4$ port at $i+4$ is 2, and finally arrives at the destination port $i+5$ at $i+5$ (the speed at arrival also is 0), and it stays at the port $i+5$ for 1 unit time. Compared with the space-time or space-speed in the two-dimensional network, the navigation process between any two ports under the space-time network is represented by space-time-speed three dimensions, which can explain the state of the liner throughout the navigation process in more detail.

In order to facilitate the construction of the model, Table 1 gives the symbols of the transportation network under the liner time-space network and their meanings. In general, (i,j) represents the transport segment of the liner from port i to port j. In the space-time network model, by introducing time and velocity dimensions, the transport section of the liner can be expressed as $(i,t,u)\rightarrow(i+\Delta i,t+\Delta t,u+\Delta u)$, where Δi, Δt and Δu represent the increment in the space distance, navigation time, and sailing speed of the liner, respectively. For easy model construction, the variation of the liner in space, time and velocity dimensions can be simplified to $(i,t,u)\rightarrow(j,s,v)$. That is, at time t, the speed u departs from port i, and the speed at which port j arrives at time s is v. Therefore, the increments in space, time and speed can be expressed as the use of a six-dimensional variable to represent the navigation process of the space-time network, namely (i,j,t,s,u,v).

Under the framework of the space-time network model, it is extremely easy to obtain the sailing speed and time of the liner between any two ports (space dimensions). In order to describe the navigation status of the liner at different times, this paper defines the space-time network liner sailing arc and the port dwell arc. The sailing arc is used to describe the course of the liner between different ports, that is, the speed and time of the liner required between the two ports. The dwell arc describes the stopping time of the liner at any port, that is, the time required for the loading and unloading of cargo and maintenance of the liner at the port. When the liner be stopped in the port, its spatial position and speed will not change and the speed is 0. Only the time is changing. Therefore, the dwell arc of the liner at any port can be expressed as $(i,i,t,s,0,0)$.

Figure 2 shows the three emission control areas in China's seas. From top to bottom, they are the ship emission control areas in the Bohai Sea, the Yangtze River Delta and the Pearl River Delta. In the emission control area, in order to meet lower emission requirements, liners often need to replace the higher-priced clean fuel as a power source, which will further increase their operating costs. In reality, the restricted area near the port is not a completely regular area, which makes it possible for the shipping company to reduce the transportation cost of using marine gas oil (MGO). In other words, the liner will choose different location of entering and leaving the control area. That is, there are a variety of options available for liner selection when navigating between any two ports. In order to illustrate the relationship between the optional link scheme and the route of the liner in the context of ECA, Figure 3 shows those relationship. Figure 3 (a) is a navigation route, that is, the order in which the liner visits the port in one service. In addition, the link between any two ports is defined as a link. Due to the existence of ECA in any ports, there may be multiple link options between any two ports for the liner selection, as shown in Figure 3 (b), between ports 1 and 2 there are three different link options. As can be seen from Figure 3, a feasible route consists of multiple links. Between ports 1 and 5, the route consists of 4 links. In this paper, it is assumed that there are three different link options between any two ports. Options 1, 2 and 3 represent the shortest distance, the shortest ECA and the longest ECA, respectively.

Table 1. *Space-time-speed network framework symbols and meaning.*

symbols	meaning
N	Set of nodes/ports
L	Set of links
H	Set of time stamps in the planning time horizon
V	Set of speed values
Q	Set of STS vertices
A	Set of STS arcs
i,j	Index of ports, $i,j\in N$, i',j' is the virtual node index
t,s	Index of time, $t,s\in H$, t',s' is the virtual time index
u,v	Values of instantaneous speed, $u,v\in V$, u',v' is the instantaneous speed value of the virtual node
(i,j)	Physical link index, $(i,j)\in L$
$(i,t,u),(j,s,v)$	Index of STS vertices, $(i,t,u),(j,s,v)\in Q$
(i,j,t,s,u,v)	Index of STS arcs indicating t departs at node i at speed u and arrives at node j at speed v at time s, arc $(i,j,t,s,u,v)\in A$

Figure 2. *Schematic diagram of the ECA in the Chinese sea area.*

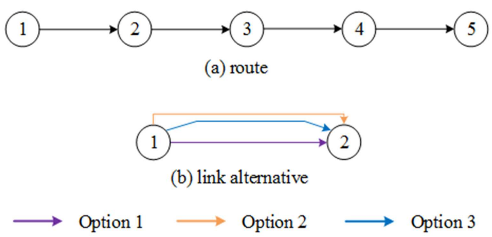

Figure 3. *Schematic diagram of the route and options link between ports.*

In order to indicate the sailing arc of the liner under the STS network, the location where the liner enters and leaves the ECA can be regarded as a virtual node, and the route between any two ports can be composed of two parts, namely, sailing within the ECA and sailing outside the ECA. Figure 4 shows a feasible navigation route between the $i-$th port and the $j-$th port, $i^{'}$ and $j^{'}$ (namely, virtual nodes) represent the nodes of the ship leaving and entering the port emission control area, respectively. Therefore, the route of the liner sailing between any two ports can be expressed as $\left(i,i^{'}\right)\rightarrow\left(i^{'},j^{'}\right)\rightarrow\left(j^{'},j\right)$, where link $\left(i,i^{'}\right)$ and $\left(j^{'},j\right)$ represent sailing within ECA, and $\left(i^{'},j^{'}\right)$ represent sailing outside ECA. Furthermore, the sailing route of the liner under the space-time-speed (STS) network model framework between any two ports can be expressed as $\left(i,i^{'},t,t^{'},u,u^{'}\right)\rightarrow\left(i^{'},j^{'},t^{'},s^{'},u^{'},v^{'}\right)\rightarrow\left(j^{'},j,s^{'},s,v^{'},v\right)$.

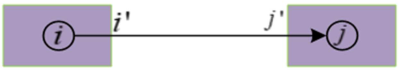

Figure 4. *Schematic diagram of the route between ports in the ECA background.*

3. Model Construction

3.1. Model Assumptions and Symbolic Description

In the framework of space-time-speed network model, in order to get the optimal route and speed, this paper has the following assumptions.

(1) When entering the emission control area near the port, the liner can meet the port's ECA rules by switching to low-sulfur fuel, installing a gas scrubber, or using liquefied natural gas (LNG) as fuel. However, due to the need to modify the liner structure for installing the scrubber and the use of LNG, the upfront cost is higher, and the price of LNG is higher [24-27]. Therefore, this paper considers the replacement of the low sulfur fuel scheme, and assumes that the liner host uses marine gas oil (MGO) when sailing within the ECA, and heavy fuel oil (HFO) is used as a fuel outside the ECA.

(2) Since the main consideration in this paper is the impact of the emission control area on the selection of liner routes, in order to meet the service frequency of liner transportation, the liner's dwell time at any port is required, but it is not necessary to consider the specific operation procedure of the liner at the port. Therefore, according to the liner transportation schedule, the liner's dwell time at each port is the same and fixed.

(3) There are three different link options available between any two ports. And under a single strategy, the link options between ports does not change, and under the hybrid strategy, the link options may change.

(4) Since the issue of liner fuel purchase is one of the other major research issues in liner transportation, it is an extremely complicated problem. As with Hypothesis 2, this paper mainly considers the impact of ECA on liner shipping routes. In order to simplify the model, the complexity of fuel purchase is not considered for the time being.

For convenience of explanation, Table 2 gives the mathematical symbol and meaning of 0-1 integer program under the space-time-speed network model framework.

Table 2. *Optimization model symbol and its meaning.*

symbol	meaning
m	Route options, $m=1,2,3$
$U_{i,j,t,s,u,v}^{m,MGO}$	Marine gas oil consumption on arc (i,j,t,s,u,v) of the $m-$th route option
$U_{i,j,t,s,u,v}^{m,HFO}$	Heavy fuel oil consumption on arc (i,j,t,s,u,v) of the $m-$th route option
$U_{i,j,t,s,u,v}^{m}$	Total fuel consumption on arc (i,j,t,s,u,v) of the $m-$th route option
$c_{r,i,j,t,s,u,v}^{m}$	Operation cost of arc (i,j,t,s,u,v) under the $m-$th route option
$x_{i,j,t,s,u,v}^{m}$	0-1 decision variable, if arc (i,j,t,s,u,v) is selected under the $m-$th route option, the value is 1; otherwise, 0.

3.2. Fuel Consumption

In order to get the operating costs of different routes, the fuel consumption rate related to speed must first be obtained. As shown in Figure 4, the fuel consumption rates for links $\left(i,i^{'}\right)$, $\left(i^{'},j^{'}\right)$ and $\left(j^{'},j\right)$ are calculated separately. Assuming that the relationship between the fuel consumption rate and the sailing speed of unit nautical mile of the liner is $g\left(v\right)=av^{b}$ [6], where a and b are parameters, the fuel consumption rate of each link in the space-time-speed network can be calculated by equation (1).

$$\begin{aligned} g_{i,i',t,t',u,u'} &= a\left(\left(u+u'\right)/2\right)^{b} \\ g_{i',j',t',s',u',v'} &= a\left(\left(u'+v'\right)/2\right)^{b} \\ g_{j',j,s',s,v',v} &= a\left(\left(v'+v\right)/2\right)^{b} \end{aligned} \tag{1}$$

Between the two ports with ECA, use $\left(i,i^{'},t,t^{'},u,u^{'}\right)$ and $\left(j^{'},j,s^{'},s,v^{'},v\right)$ to represent within the ECA arc between the $i-$th port and the $j-$th port under the STS network. $\left(u+u'\right)/2$ and $\left(v'+v\right)/2$ are the average sailing speeds within the ECA. $\left(i^{'},j^{'},t^{'},s^{'},u^{'},v^{'}\right)$ indicates outside the ECA arc, and $\left(u'+v'\right)/2$ is the average sailing speed outside the ECA. In Eq. (1), $g_{i,i^{'},t,t^{'},u,u^{'}}$ and $g_{j^{'},j,s^{'},s,v^{'},v}$ represent fuel consumption within the ECA, and $g_{i^{'},j^{'},t^{'},s^{'},u^{'},v^{'}}$ is outside.

Knowing the unit nautical mile fuel consumption rate on each potential arc and multiplying it by the actual distance between the two ports, the actual fuel consumption required can be obtained. Under STS network framework, the actual distance between any two nodes can be expressed by the speed multiplied by the time, so that the fuel consumption function with the sailing speed $b+1$ power relationship can be obtained. Then, the consumption of MGO and HFO on each arc of the space-time-speed network in the $m-$th route option can be calculated by equations (2) and (3), respectively.

$$U^{m,MGO}_{i,j,t,s,u,v} = L^{m}_{i,i'} g_{i,i',t,t',u,u'} + L^{m}_{j',j} g_{j',j,s',s,v',v} = a\left(\left(t'-t\right)\left(\frac{u+u'}{2}\right)^{b+1} + \left(s-s'\right)\left(\frac{v'+v}{2}\right)^{b+1}\right) \tag{2}$$

$$U^{m,HFO}_{i,j,t,s,u,v} = L^{m}_{i',j'} g_{i',j',t',s',u',v'} = a\left(s'-t'\right)\left(\frac{u'+v'}{2}\right)^{b+1} \tag{3}$$

Where, $L^{m}_{i,i'}$, $L^{m}_{i',j'}$ and $L^{m}_{j',j}$ are the actual distances of the link $\left(i,i'\right)$, $\left(i',j'\right)$ and $\left(j',j\right)$ under the $m-$th route option, respectively. Therefore, the total consumption on each arc under the STS network can be calculated by equation (4).

$$U^{m}_{i,j,t,s,u,v} = U^{m,MGO}_{i,j,t,s,u,v} + U^{m,HFO}_{i,j,t,s,u,v} \tag{4}$$

3.3. Transportation Costs

After knowing the specific consumption of different types of fuel on each arc, multiply by the corresponding price to get the transportation cost. Use $p^{MGO}_{i,j,t,s,u,v}$ and $p^{HFO}_{i,j,t,s,u,v}$ to indicate the price of MGO and HFO, respectively. Then the cost of the transporter on each arc of the $m-$th route option can be calculated by equation (5).

$$c^{m}_{i,j,t,s,u,v} = p^{MGO}_{i,j,t,s,u,v} U^{m,MGO}_{i,j,t,s,u,v} + p^{HFO}_{i,j,t,s,u,v} U^{m,HFO}_{i,j,t,s,u,v} \tag{5}$$

4. Optimization Model

For the shipping company, while ensuring that each route service can be completed on time, the transportation cost should be reduced as much as possible. Under the space-time network model framework, the following model can be established according to the transportation cost on each potential STS arc.

$$\min\ Z = \sum_{m=1}^{3} \sum_{(i,j,t,s,u,v)\in A} \left(c^{m}_{i,j,t,s,u,v} \cdot x^{m}_{i,j,t,s,u,v}\right) \tag{6}$$

$$\sum_{(j,s,v)\in Q} x^{m}_{i,j,t,s,u,v} - \sum_{(j,s,v)\in Q} x^{m}_{j,i,s,t,v,u} = \begin{cases} 1 & i=o, t=edt, v=0 \\ -1 & i=d, t=lat, v=0 \\ 0 & otherwise \end{cases} \tag{7}$$

$$\sum_{(i,j,t,s,u,v)\in A} \left(x^{m}_{i,j,t,s,u,v} \cdot (s-t)\right) \le T \tag{8}$$

$$U^{m,MGO} = \sum_{(i,j,t,s,u,v)\in A} \left(U^{m,MGO}_{i,j,t,s,u,v} \cdot x^{m}_{i,j,t,s,u,v}\right) \tag{9}$$

$$U^{m,HFO} = \sum_{(i,j,t,s,u,v)\in A} \left(U^{m,HFO}_{i,j,t,s,u,v} \cdot x^{m}_{i,j,t,s,u,v}\right) \tag{10}$$

$$\sum_{(i,j,t,s,u,v)\in A} x^{m}_{i,j,t,s,u,v} = 1 \quad \forall i = j \tag{11}$$

$$x^{m}_{i,j,t,s,u,v} \in \{0,1\} \quad (i,j,t,s,u,v)\in A, m = 1,2,3 \tag{12}$$

Eq. (6) is the objective function that minimizes operating costs. $x^{m}_{i,j,t,s,u,v}$ is a 0-1 decision variable. If the STS arc (i,j,t,s,u,v) is selected for navigation under the $m-$th route option, the value is 1, otherwise 0. Eq. (7) – Eq. (12) is a constraint, Where Eq. (7) is the time-space network equilibrium flow constraint, o and d are the origin port and destination port in a service, edt and lat are the earliest departure time and the latest arrival time to complete a service; Eq. (8) is the time constraint required for navigation services, and T is the total service time for one voyage; Eq. (9) and Eq. (10) calculate the consumption of MGO and HFO in navigation respectively; Eq. (11) constrains the liner must dwell in any port; Eq. (12) is the 0-1 constraint of the decision variable.

5. Empirical Analysis

In order to explain the impact of emission control area on liner operating cost and optimal route selection, this paper studies from two aspects: single line strategy and hybrid route strategy. Under the single strategy, the liner chooses a solution to complete the voyage, i.e. the shortest distance, the shortest ECA or the longest ECA. Under the hybrid strategy, the liner may choose a variety of options to complete the voyage, that is, joint optimization of multiple options. Under the spatio-temporal network model, the 0-1 integer programming model constructed by discretizing the speed is solved based on the MATLAB 2015b platform using the YALMIP modeling language to call the CPLEX solver.

5.1. Fuel Price and Route Selection

Table 3 gives an overview of the validation model case. Due to the different sailing distances under different route schemes, the arrival time of different schemes is different under STS network. There are a variety of routes to choose from port-to-port. The problem to be considered in the hybrid strategy is that in the case of minimizing operating costs, any two adjacent ports will choose which type of options to navigate. Therefore, the travel distance is unknown when the solution is not solved. For ease of description, the hybrid strategy is defined as Option 4.

Table 3. *Overview of each case.*

Case	Route	Port within ECA	Options	Distance (nautical)		Departure and arrival time (hour)
				Within ECA	Outside ECA	
1	Busan-Shanghai-Busan	Shanghai	1	110	740	1, 58
			2	90	792	1, 57
			3	230	724	1, 61
			4	-	-	1, 67
2	Hong Kong-Hai Phong-Yantian	Hong Kong, Yantian	1	332	632	1, 62
			2	92	948	1, 63
			3	405	628	1, 64
			4	-	-	1, 76
3	Shanghai-Hong Kong-Hai Phong	Shanghai, Hong Kong	1	426	804	1, 75
			2	135	1262	1, 73
			3	572	788	1, 88
			4	-	-	1, 95
4	Xingang-Shanghai-Hong Kong	Xingang, Shanghai, Hong Kong	1	590	882	1, 74
			2	381	1202	1, 69
			3	739	839	1, 82
			4	-	-	1, 105

The three routes of Cases 1, 2, and 3 were provided by COSCO. Case 1 is a South Korean route. After departing from Busan, South Korea, via Shanghai, China, it will eventually return to Busan, South Korea. The Chinese Shanghai Port is within the ECA. Cases 2 and 3 are the Thailand-Vietnam routes. The case 2 route is from China Hong Kong to Vietnam's Hai Phong and returns to China's Yantian. Two ports of this routes are within ECA, namely, Hong Kong and Yantian, China; Case 3's route from Shanghai, China, arrived in Vietnam's Haiphong after passing through Hong Kong, China. It is the same as Case 2, in which two ports of Shanghai and Hong Kong are within ECA. Case 4 is a domestic route from Xingang to Shanghai after arriving in Hong Kong. The three ports on the route are all within the ECA. Based on the previous assumptions, the liner's dwell time at each port is set to 6 hours.

The prices of fuel are a major input parameter to the model and vary from port to port and often change. The problem considered in this paper is the impact of the emission control area on the route. Therefore, the average value of the weekly price data of Shanghai Port and Singapore Port since 2018 is used as the input value, in which the price of MGO is 688.89 US dollars / ton, and the price of HFO is 438.10 US dollars / ton.

The fuel consumption rate is not only related to the sailing speed of the liner, but also related to the capacity of the liner and the sea conditions of the port-to-port. The research about the relationship between the fuel consumption rate and sailing speed has been very detailed. According to Wang and Meng's research on the parameters of historical fuel consumption and sailing speed data of different types of liners, it is generally considered that the exponent is between 2.7 and 3.3 [6]. This paper mainly considers the impact of ECA on liner route selection. Therefore, the exponent relationship between fuel consumption rate and speed is based on the fitting results of Wang and Meng parameters. The average value of the parameters under 5000 TEU is used as the fuel consumption rate parameter, i.e. $a = 0.013, b = 2.712$ [28].

Moreover, under the STS network, by discretizing the speed with a reasonable step size, the fuel consumption rate can be simply regarded as a constant, and the nonlinear programming model when it is used as a decision variable can be avoided to facilitate the model solving. The set of speeds considered in this paper is $V = [18,19,20,21,22]$.

5.2. Analysis of Empirical Results

Under the hybrid strategy, the liner route plan is dynamically changed, and different options are selected for navigation between different ports. Table 4 shows the selection of the best options and the actual voyage distance between different ports under the hybrid strategy for each case.

Table 4. *Distance port-to-port in each case.*

Case	Link	Option 1		Option 2		Option 3		Option 3		
		IN	OUT	IN	OUT	IN	OUT	IN	OUT	Option
1	Busan-Shanghai	55	370	45	396	115	362	55	370	1
	Shanghai-Busan	55	370	45	396	115	362	45	396	2
	total distance (nautical)	110	740	90	792	230	724	100	766	-
		850		882		954		866		
2	Hong Kong-Hai Phong	144	316	38	468	183	314	38	468	2
	Hai Phong-Yantian	188	316	54	480	222	314	188	316	1
	total distance (nautical)	332	632	92	948	405	628	226	784	-

Case	Link	Option 1		Option 2		Option 3		Option 3		
		IN	OUT	IN	OUT	IN	OUT	IN	OUT	Option
		964		1040		1033		1010		
3	Shanghai-Hong Kong	273	496	92	796	377	492	273	496	1
	Hong Kong-Hai Phong	153	308	43	466	195	296	43	466	2
	total distance (nautical)	426	804	135	1262	572	788	316	962	-
		1230		1397		1360		1278		
4	Xingang-Shanghai	292	388	270	407	349	343	349	343	3
	Shanghai-Hong Kong	298	494	111	795	390	496	111	795	1
	total distance (nautical)	590	882	381	1202	739	839	460	1138	-
		1472		1583		1578		1598		

Note: IN indicates the condition of the liner sailing within the ECA, and OUT means outside the ECA.

It can be seen from Table 4 that the navigation schemes among the ports under the hybrid strategy are different in different cases. The shortest distance and the shortest ECA in Case 1 and Case 3 are the best hybrid schemes. The shortest ECA and the shortest distance in Case 2 are the best schemes. In Case 4, the longest ECA and the shortest ECA are the best hybrids. From the perspective of the total navigation distance, Case 4 has the longest sailing distance under the hybrid strategy, while in the other three cases, the hybrid strategy's sailing distance is second only to the shortest distance. Moreover, in addition to the shortest ECA, the hybrid strategy is the one with the shortest sailing distance within the ECA, which means that the liner will dynamically select the route plan during the driving process.

Different schemes will result in different transportation costs during the voyage. Figure 5 shows the minimum transportation costs for different route scenarios in four cases. Since the route schemes in Case 1 are significantly smaller than other cases, the transportation cost is also the smallest among the four cases. In contrast, the longest Case 4 under each option has the highest transportation costs. The minimum operating costs under the optimal route schemes for Cases 1, 2, 3, and 4 were 131674.89 USD, 200411.44USD, 204043.52USD, and 266213.93USD, respectively.

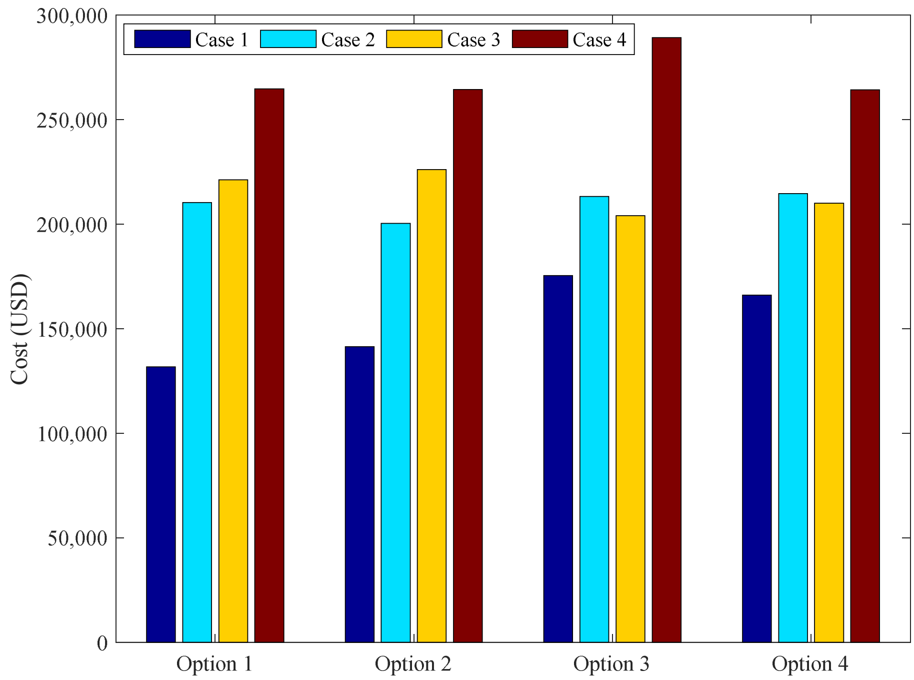

Figure 5. *Transportation costs of different route schemes under each case.*

As can be seen from Figure 5, the route option for the minimum transportation cost in different cases is different. In Case 1, Option 1 is clearly superior to the other options. In this case, there is one port within the ECA, and the total distance of the shortest distance navigation is significantly smaller than other options. In Case 2, although the total navigation distance of the Option 2 is longer, but the distance traveled within the ECA is significantly smaller than other options, so the Option 2 is optimal. Although the navigation distance of the Option 3 within the ECA is longer, the distance traveled outside the ECA is much smaller than other options, and the navigation distance in the ECA is complementary, forming the most route scheme under the Case 3. In Case 4, the ports of the route are all within the ECA, and the total navigation distance difference under each option is small. The sailing distance in the ECA is significantly smaller than the Option 1 and Option

3, and compared with Option 2, the driving distance inside and outside the ECA is relatively close. Therefore, the hybrid strategy (Option 4) is the optimal route option in this case.

It can be seen from the above analysis that in the context of ECA, the influence of the number of ports within the ECA on different distances and routes on the transportation cost is extremely obvious. Moreover, the transportation cost is related to the fuel consumption during the navigation. Table 5 shows the fuel consumption of different route schemes in each case. Due to the different prices of marine gas oil and heavy fuel oil, the total fuel consumption of the optimal route plan in each case is not necessarily the smallest. It can be seen from Table 5 that the optimal fuel consumption of the best solutions in Cases 1 and 3 is the smallest, and the consumption of heavy fuel oil is the smallest in Case 1. In Case 3, since the optimal solution is the longest ECA, the consumption of marine gas oil is the largest, but at the same time, the distance traveled outside the ECA is small, and the consumption of heavy fuel oil is much smaller than other options. Case 2 is similar to Case 4, and the consumption of a small amount of marine gas oil offsets the transportation cost of a large amount of heavy fuel oil consumption.

Table 5. *Fuel consumption of different route options under each case (Ton).*

Case	Optimal option		Option 1	Option 2	Option 3	Option 4
		MGO	44.14	29.02	105.20	35.36
1	Option 1	HFO	231.15	277.14	234.95	323.49
		Sum	275.29	306.16	340.15	358.85
		MGO	140.44	67.09	184.39	106.55
2	Option 2	HFO	259.20	351.97	196.73	322.23
		Sum	399.64	419.06	381.12	428.78
		MGO	185.01	75.02	196.56	100.92
3	Option 3	HFO	214.08	398.18	156.67	320.56
		Sum	399.09	473.20	353.23	421.48
		MGO	262.16	186.77	303.97	130.60
4	Option 4	HFO	191.91	309.97	182.29	397.73
		Sum	454.07	496.74	486.26	528.33

Table 6. *Average speed of the optimal option in each case.*

Case	Optimal option	Link	Time (hours)		Speed (knots)	
			Within ECA	Outside ECA	Within ECA	Outside ECA
1	Option 1	Busan-Shanghai	3	17	20	21.5
		Shanghai-Busan	3	21	18	18
2	Option 2	Hong Kong-Hai Phong	2	22	22	21.25
		Hai Phong-Yantian	3	23	21	21
3	Option 3	Shanghai-Hong Kong	20	27	18.5	18.5
		Hong Kong-Hai Phong	11	16	18	18
4	Option 4	Xingang-Shanghai	19	19	19	19
		Shanghai-Hong Kong	6	42	18.5	18.5

Note: The sailing time is rounded off.

The fuel consumption per unit distance is also related to the sailing speed. Table 6 shows the average speed port-to-port under the optimal solution in each case. It can be seen from Table 6 that in different cases, the speed of the liner within the ECA is generally low, in order to save the consumption of MGO. However, in order to ensure that the service is completed on time, the speed of navigation outside the ECA is higher. In Cases 3 and 4, the average speed of the liner is the same inside and outside the ECA, depending on the longest ECA and the hybrid strategy the sailing distance. It can be seen from Table 4 that since the optimal solution of Case 3 is the longest ECA, the distance between the inside and outside of the ECA is relatively close, so the speed is relatively close. In Case 4, the navigation distance and the service time is relatively long, so the navigation speed is low in the whole process.

In the space-time-speed network model framework, it is easy to get the liner route and timetable. Figure 6 shows the route diagram of the optimal solution in each case. It can be clearly seen from Figure 6 that the optimal route options for Cases 1, 2, 3, and 4 are the shortest distance, the shortest ECA, the longest ECA, and the hybrid strategy, respectively. It can be seen from Case 4 that when all ports on the route are in the emission control area, the optimal route option for the liner should be dynamic, that is, different schemes should be selected between different ports. In the case (Case 4) given in this paper, there are two links between the three ports, so there are two best options involved, the best solution between Xingang and Shanghai is the longest ECA, and the shortest ECA between Shanghai and Hong Kong is chosen to minimize the consumption of MGO in order to minimize transportation costs.

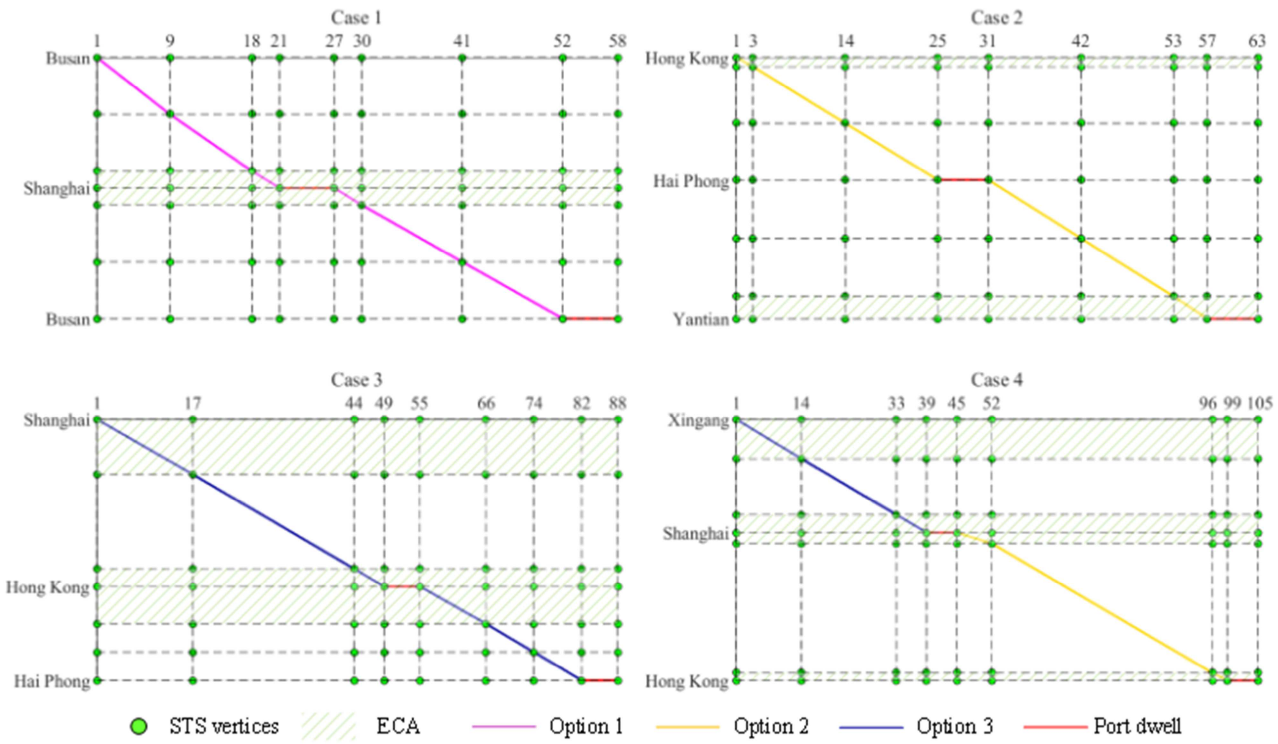

Figure 6. *Schematic diagram of the optimal route option in each case.*

6. Conclusion

In the context of a port emission control area, liners often need to replace higher-priced low-sulfur fuels in order to meet lower emission requirements within the ECA, which further increases the cost of shipping liners. The driving distance in different ECAs will directly affect the consumption of low-sulfur fuel by the liner, which will affect the cost of the entire transportation process. Therefore, this paper comprehensively considers the fuel consumption and port emission control area factors, with the goal of minimizing the cost of liner shipping, and optimizes the problem of liner routes when there are multiple route options port-to-port, and constructs cases in different situations for comparative analysis. The research results show that the choice of liner route is different under different circumstances. When there are fewer ports within the ECA on one route, it is the best solution to navigate with the shortest distance, such as Case 1. However, when multiple ports are in the ECA, the shortest distance is not necessarily the optimal solution. The liner may choose the shortest ECA scheme or even the longest ECA scheme, such as Case 2 and Case 3. When each port visited by the liner is in the ECA, the optimal route plan of the liner is dynamic, and the choice between the two ports is not fixed, that is, the hybrid strategy is its optimal solution. The three ports in Case 4 given in this paper have emission control requirements. From the optimization results, it has different route schemes between any two ports. For example, the longest ECA option is selected from the navigation from Xingang to Shanghai, and the shortest ECA from Shanghai to Hong Kong is the best choice.

Based on the background of the emission control area, the study of the optimal fueling port selection under the liner multi-route scheme and the specific gas emissions inside and outside the ECA and the impact of the price of different types of fuel on the selection of liner routes are the main directions in future research.

References

[1] UNCTAD. 2018. Review of Maritime Transportation. 2018 [EB/OL]. (accessed 2019-03-05). <https://unctad.org/en/PublicationsLibrary/rmt2018_en.pdf>.

[2] Notteboom, T. E., Vernimmen, B., 2009. The effect of high fuel costs on liner service configuration in container shipping [J]. Journal of Transport Geography, 17 (5), 325-337.

[3] Ronen, D., 1982. The effect of oil price on the optimal speed of ships. Journal of the Operational Research Society, 33 (11), 1035-1040.

[4] Ronen, D., 2011. The effect of oil price on containership speed and fleet size [J]. Journal of the Operational Research Society, 62 (1), 211-216.

[5] Schinas, O., Stefanakos, C., 2012. Cost assessment of environmental regulation and options for marine operators [J]. Transportation Research Part C: Emerging Technologies, 25, 81–99.

[6] Wang, S., Meng, Q., 2012. Sailing speed optimization for container ships in a liner shipping network [J]. Transportation Research Part E: Logistics & Transportation Review, 48 (3), 701-714.

[7] Kontovas, C., Psaraftis, H. N., 2011. Reduction of emissions along the maritime intermodal container chain: operational models and policies [J]. Maritime Policy & Management, 38 (4), 451-469.

[8] Psaraftis, H. N., Kontovas, C. A., 2013. Speed models for energy-efficient maritime transportation: a taxonomy and survey [J]. Transportation Research Part C: Emerging Technologies, 26 (26), 331-351.

[9] Psaraftis, H. N., Kontovas, C. A., 2009. CO2 emissions statistics for the world commercial fleet [J]. WMU Journal of Maritime Affairs, 8 (1), 1–25.

[10] Psaraftis, H. N., Kontovas, C. A., 2010. Balancing the economic and environmental performance of maritime transportation [J]. Transportation Research Part D: Transport & Environment, 15 (8), 458–462.

[11] Qi, X., Song, D. P., 2012. Minimizing fuel emissions by optimizing vessel schedules in liner shipping with uncertain port times [J]. Transportation Research Part E: Logistics and Transportation Review, 48 (4), 863–880.

[12] Lindstad, H., Eskeland, G. S., 2016. Environmental regulations in shipping: policies leaning towards globalization of scrubbers deserve scrutiny [J]. Transportation Research Part D: Transport & Environment, 47, 67–76.

[13] IMO, 2018. International Maritime of Organization Website. (accessed 25.03.2019). <http://www.imo.org/en/OurWork/Environment/PollutionPrevention/AirPollution/Pages/Air-Pollution.aspx>.

[14] Cheng, W. T., Zhang, H. C., 2017. Sulfur emissions control area and carbon emission reduction under the liner route optimization research [J]. Journal of central China Normal University (Nat. Sci.), 51 (5): 663-670.

[15] Jin, Z. H., Hu, J., Yang, Y. Z., et al. 2009. Optimization on voyage scheduling for container feeder lines [J]. Journal of Dalian Maritime University, 35 (3): 32-36.

[16] Schinas, O., Stefanakos, C. N., 2012. Cost assessment of environmental regulation and options for marine operators [J]. Transportation Research Part C: Emerging Technologies, 25 (8), 81-99.

[17] Cullinane, K., Bergqvist, R., 2014. Emission control areas and their impact on maritime transport [J]. Transportation Research Part D: Transport & Environment, 28, 1-5.

[18] Jiang, L., Kronbak, J., Christensen, L. P., 2014. The costs and benefits of Sulphur reduction measures: Sulphur scrubbers versus marine gas oil [J]. Transportation Research Part D: Transport & Environment, 28 (2), 19-27.

[19] Yang, Z. L., Zhang, D., Caglayan, O., Jenkinson, I. D., Bonsall, S., Wang, J., et al. 2012. Selection of techniques for reducing shipping NOx and Sox emissions [J]. Transportation Research Part D: Transport & Environment, 17 (6), 478-486.

[20] Brynolf, S., Magnusson, M., Fridell, E., Andersson, K., 2014. Compliance possibilities for the future ECA regulations through the use of abatement technologies or change of fuels [J]. Transportation Research Part D: Transport & Environment, 28 (5), 6-18.

[21] Balland, O., Erikstad, S. O., Fagerholt, K., 2012. Optimized selection of air emission controls for vessels [J]. Maritime Policy & Management, 39 (4), 387-400.

[22] Balland, O., Fagerholt, K., Wallace, S. W., 2013. Planning vessel air emission regulations compliance under uncertainty [J]. Journal of Marine Science & Technology, 18 (3), 349-357.

[23] Fagerholt, K., Gausel, N. T., Jorgen, G., et al. 2015. Maritime routing and speed optimization with emission control areas [J]. Transportation Research Part C: Emerging Technologies, 52: 57-73.

[24] Gu, Y., Wallace, S. W., 2017. Scrubber: a potentially overestimated compliance method for the emission control areas [J]. Transportation Research Part D: Transport and Environment, 55, 51-66.

[25] Balland, O., Erikstad, S. O., Fagerholt, K., Wallace, S. W., 2013. Planning vessel air emission regulations compliance under uncertainty [J]. Journal of Marine Science and Technology 18 (3), 349–357.

[26] Boscaratoa, I., Hickeya, N., Kašpara, J., Pratib, M. V., Mariani, A., 2015. Green shipping: Marine engine pollution abatement using a combined catalyst/seawater scrubber system. 1. Effect of catalyst [J]. Journal of Catalysis, 328, 248–257.

[27] Doudnikoff, M., Lacoste, R., 2014. Effect of a speed reduction of containerships in response to higher energy costs in Sulphur Emission Control Areas [J]. Transportation Research Part D: Transport & Environment, 28, 51–61.

[28] Wang, S. A., Wang, X. C., 2016. A polynomial-time algorithm for sailing speed optimization with containership resource sharing [J]. Transportation Research Part B: Methodological, 93: 394-405.